18

A Model-Based Synthetic Approach to the Dynamics, Guidance, and Control of AUVs

Kangsoo Kim and Tamaki Ura
NTT Communication Science Laboratories, Nippon Telegraph and Telephone Corporation
Institute of Industrial Science, The University of Tokyo

1. Introduction

In this article, we present a model-based synthetic approach applied to the dynamics, guidance, and control of Autonomous Underwater Vehicles (AUVs). The feature of vehicle dynamics is one of the most important concerns in designing and developing an AUV, while the guidance and control are the key issues in fulfilling the vehicle performance. Our approach deals with these individual but closely interrelated issues in a consistent way based on the model-based simulations.

In our research, as the dynamic model of an AUV, we employ a set of equations of motion describing the coupled 6-D.O.F. behaviour in 3-D space. In the linearized form of the equations of motion derived on the basis of the small perturbation theory, to complete the dynamic model of an AUV we have to determine so called stability derivatives or hydrodynamic coefficients of the AUV. In general, determination of the stability derivatives requires quite amount of effort and time, since they are functions of the fluid dynamic loads depending on the vehicle motion (Etkin, 1982; Lewis et al., 1989). There are many, well-established approaches for determining stability derivatives of the air vehicles (McRuer et al., 1990; Etkin, 1982) or the marine vehicles (Lewis et al., 1989), which are based on either experiment or theoretical prediction. While the experimental approach allows direct measurement of the fluid dynamic forces and moments acting on the vehicle, it requires large amount of time, labour, expense, as well as the experimental facility. On the other hand, nowadays a few state-of-the-art techniques are available in predicting the stability derivatives theoretically. Most of them are however specialized in deriving the stability derivatives for the dynamics of conventional airplane or ship, hard to be directly applied to the modelling problems related to a specific AUV dynamics. In this respect, we present a technique of deriving the dynamic model of an AUV mainly on the basis of the CFD (Computational Fluid Dynamics) analyses, which is applicable to any kind of vehicle moving in a fluid environment. In our approach based on this technique, we determine some stability derivatives dominating the dynamics of an AUV by differentiating the hydrodynamic loads obtained from the CFD analyses.

The derived dynamic model is directly applied to the model-based design of the motion control systems of a vehicle. Two PID type low-level controllers are employed to let a

vehicle follow the desired trajectories in the longitudinal and the lateral sections, represented by time sequences of the depth (altitude) and the heading.

As an intelligent high-level control of AUVs, a strategy of optimal guidance in current disturbance is presented. Suppose that a vehicle is to transit to a given destination in a region of environmental disturbance. Then it is quite natural that navigation time of the vehicle should change according to the selection of a specific trajectory. The optimal guidance proposed in this research is the minimum-time guidance in sea current environments, letting a vehicle reach a destination with the minimum travel time. When the power consumption of an AUV is controlled to be constant throughout the navigation, the navigation time is directly proportional to the total energy consumption. Released from the umbilical cable, an AUV has to rely on restricted energy stores during the undersea mission. Therefore for an AUV, minimizing navigation time offers an enhanced potential for vehicle safety and mission success rate.

We present a numerical procedure deriving the optimal heading reference by tracking which a vehicle achieves the minimum-time navigation in a given sea current distribution. The proposed procedure for implementing the optimal guidance is systematic and works in any deterministic current field whether stationary or time-varying. Moreover, unlike other path-finding algorithms such as Dynamic Programming (DP) or Generic Algorithm (GA) (Alvarez et al., 2004), our procedure does not require computation time increase for the time-varying problem.

In real environments of AUV navigation, there are some factors which can cause the failure in realizing the proposed optimal guidance strategy (Kim & Ura, 2008). Some examples of such factors are environmental uncertainties in sea currents, severe sensor noises, or temporally-faulty actuators. As a fail-safe strategy in realizing the optimal or minimum-time navigation, we present the concept of quasi-optimality. Basic idea of the quasi-optimal navigation is quite simple. It consists of repetitive revisions of the optimal heading reference in respond to the on-site request of the optimal guidance revision for preventing from the failure in on-going optimal navigation. The quasi-optimal navigation has practical importance since in real sea environments, there actually are several possible actions which deteriorate the realization of the optimal navigation.

2. An AUV "R-One"

In this article, we practice our strategy in dynamics, guidance, and control on an AUV "R-One". The R-One is a long-range cruising type AUV, developed by the Institute of Industrial Science (IIS), the University of Tokyo. Figure 1 shows overall layout of the R-One.

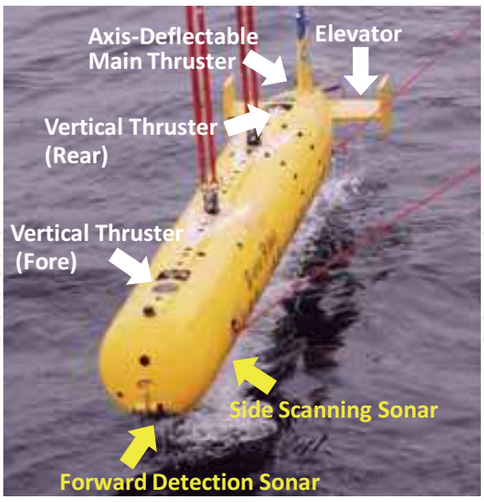

Fig. 1. Overall layout of the long-range cruising type AUV R-One.

Figure 2 shows the coordinate system and the actions of actuators installed in the R-One. While the axis-deflectable main thruster keeps and changes the vehicle's kinematic states in horizontal plane, two elevators and two vertical thrusters play the same role in vertical plane.

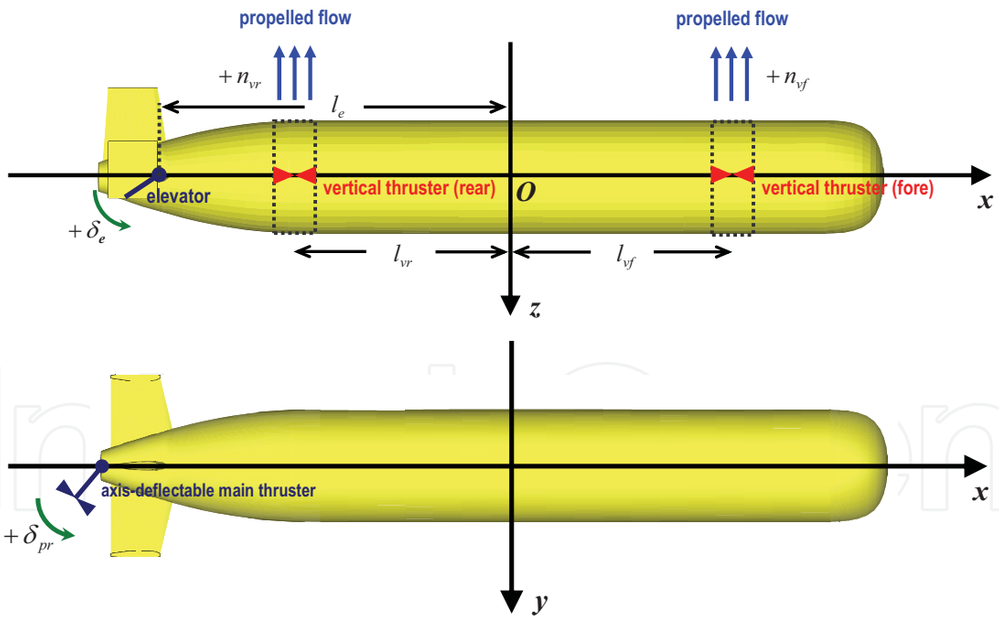

Fig. 2. Coordinate system and actuator actions in describing the dynamics of R-One. The coordinate system takes its origin at the center of gravity of the vehicle. n_{vf} and n_{vr} are the rpms of fore and rear vertical thrusters. δ_e is the elevator deflection.

3. Modelling Vehicle Dynamics

3.1 Equations of Motion for Vehicle Dynamics

The equations of motion describing the vehicle motion mathematically can be derived from the conservation law of the linear and the angular momenta with respect to the inertial frame of reference. If the axes of reference frame are nonrotating however, it should be noted that as the vehicle rotates, mass moments and products of inertia will vary, thus the time derivatives of them appear explicitly in the equations of motion (McRuer et al., 1990; Etkin, 1982). This increases the mathematical complexity which causes serious interference in treating the equations numerically as well as analytically. This is why the most of equations of motion of a rigid body in 3-D space are defined with respect to the body-fixed frame of reference. In (1), equations of motion describing the 6-D.O.F. motion of an AUV are shown. The equations are defined with respect to the body-fixed frame of reference shown in Fig. 3, in which the origin is taken at the vehicle's center of gravity.

$$m(\dot{U} + QW - RV) = -(m - \rho\nabla)g\sin\Theta + X \tag{1a}$$

$$m(\dot{V} + RU - PW) = (m - \rho\nabla)g\cos\Theta\sin\Phi + Y \tag{1b}$$

$$m(\dot{W} + PV - QU) = (m - \rho\nabla)g\cos\Theta\cos\Phi + Z \tag{1c}$$

$$I_{xx}\dot{P} - I_{xz}\dot{R} - I_{xz}PQ + (I_{zz} - I_{yy})QR = \rho\nabla g z_B \cos\Theta\sin\Phi + L \tag{1d}$$

$$I_{yy}\dot{Q} + (I_{zz} - I_{zz})RP + I_{xz}(P^2 - R^2) = \rho\nabla g z_B \sin\Theta + M \tag{1e}$$

$$-I_{xz}\dot{P} + I_{zz}\dot{R} + (I_{yy} - I_{xx})PQ + I_{xz}QR = N \tag{1f}$$

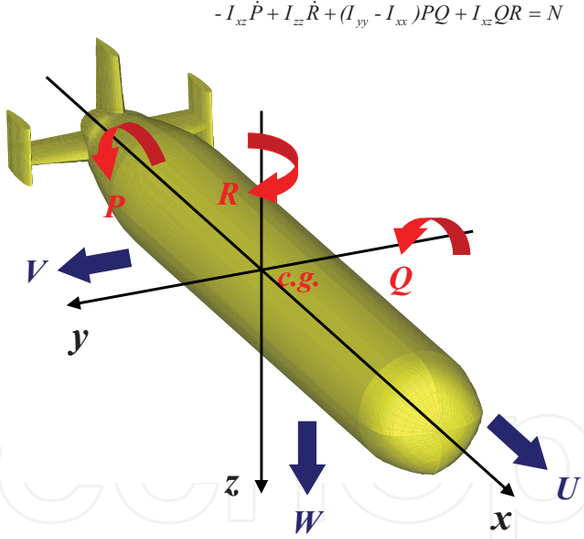

Fig. 3. Body-fixed coordinate system with linear and angular velocity components.

In (1), *U*, *V*, *W*, and *P*, *Q*, *R* are *x*, *y*, *z* components of linear and angular velocities. ∇, *M*, and *I* represent displacement, mass, and mass moments or products of inertia of a vehicle. ρ and g are constants expressing water density and gravitational acceleration. Hydrodynamic forces and moments are represented by *X*, *Y*, *Z*, and *L*, *M*, *N*, each of which is the component in the direction of *x*, *y*, *z*. Φ, Θ, and Ψ are so called Euler angles to be defined in the coordinate transformation between the body-fixed and the inertial frames of reference. z_B is the z-directional displacement of the buoyancy center of the vehicle. Eqs. (1) are quite

similar to those describing the dynamics of the aircraft. It should be noted that however, terms expressing the hydrostatic forces and moments do not appear in the equations for aircraft dynamics.

The equations of motion are frequently linearized for use in stability and control analysis as remarked in Etkin (1982) or McRuer et al. (1990). The equations are linearized on the basis of the small perturbation theory in which it is assumed that the motion of the vehicle consists of small deviations from a reference condition of steady motion. Equations (2) are the linearized form of the Eqs. (1), in which u, v, w, p, q, r, ϕ, θ, and ψ denote small amounts of velocities and displacements perturbed from their reference values which are expressed by their uppercase letters.

$$m(\dot{u} + qW_0) = -\theta(m - \rho\nabla)g\cos\theta_0 + X \tag{2a}$$

$$m(\dot{v} + rU_0 - pW_0) = \phi(m - \rho\nabla)g\cos\theta_0 + Y \tag{2b}$$

$$m(\dot{w} - qU_0) = -\theta(m - \rho\nabla)g\sin\theta_0 + Z \tag{2c}$$

$$I_{xx}\dot{p} - I_{xz}\dot{r} = \phi\rho\nabla g z_B \cos\theta_0 + L \tag{2d}$$

$$I_{yy}\dot{q} = \theta\rho\nabla g z_B \cos\theta_0 + M \tag{2e}$$

$$-I_{xz}\dot{p} + I_{zz}\dot{r} = N \tag{2f}$$

$$\dot{\phi} = p + r\tan\theta_0 \tag{2g}$$

$$\dot{\theta} = q \tag{2h}$$

$$\dot{\psi} = r\sec\theta_0 \tag{2i}$$

To complete the linearized equations of motion for the use in stability and control analysis, hydrodynamic loads are expanded and linearized on the assumption that they are functions of the instantaneous values of the perturbed velocities, control inputs, and their derivatives. Thus the expressions of the hydrodynamic loads are obtained in the form of a Taylor series in these variables, which is linearized by discarding all the higher-order terms. For example, X is expanded as

$$X = X_u u + X_w w + X_{\dot{u}}\dot{u} + X_{n_m} n_m \tag{3}$$

where

$$X_u = \left.\frac{\partial X}{\partial u}\right)_0, \quad X_w = \left.\frac{\partial X}{\partial w}\right)_0, \text{ etc.}$$

The subscript zero indicates a reference condition where the derivatives are evaluated. In (3), the derivatives such as X_u or X_w are called stability derivatives. By expanding all the external hydrodynamic loads introducing stability derivatives of dynamical correlations, the equations of motion (2) are expressed by means of the stability derivatives as

$$(m - X_{\dot{u}})\dot{u} + mW_0\dot{\theta} - X_u u - X_w w + \theta(\rho\nabla - m)g\cos\theta_0 = X_{n_m} n_m \tag{4a}$$

$$(m - Z_{\dot{w}})\dot{w} - Z_{\dot{q}}\dot{q} - Z_u u - Z_w w - (mU_0 + Z_q)q - \theta(\rho\nabla - m)g\sin\theta_0 = Z_{n_{Vf}} n_{Vf} + Z_{n_{Vr}} n_{Vr} + Z_{\delta e}\delta_e \tag{4b}$$

$$-M_{\dot{w}}\dot{w} + (I_{yy} - M_{\dot{q}})\dot{q} - M_u u - M_w w - M_q q - \theta\rho\nabla g z_B \cos\theta_0 = -Z_{n_{Vf}} l_{vf} n_{Vf} + Z_{n_{Vr}} l_{vr} n_{Vr} + Z_{\delta e} l_{\delta_e}\delta_e \tag{4c}$$

$$(m - Y_{\dot{v}})\dot{v} - Y_{\dot{r}}\dot{r} - Y_v v - (mW_0 + Y_p)p + (mU_0 - Y_r)r = Y_{\delta_{pr}}\delta_{pr} \tag{4d}$$

$$-L_{\dot{v}}\dot{v} + (I_{xx} - L_{\dot{p}})\dot{p} - (I_{xz} + L_{\dot{r}})\dot{r} - L_v v - L_p p - L_r r - \phi\rho\nabla g z_B \cos\theta_0 = L_{\delta_{pr}}\delta_{pr} \quad (4e)$$

$$-N_{\dot{v}}\dot{v} + (I_{xz} + N_{\dot{p}})\dot{p} + (I_{zz} - N_{\dot{r}})\dot{r} - N_v v - N_p p - N_r r = N_{\delta_{pr}}\delta_{pr} \quad (4f)$$

$$\dot{\phi} = p + r\tan\theta_0 \quad (4g)$$

$$\dot{\theta} = q \quad (4h)$$

$$\dot{\psi} = r\sec\theta_0 \quad (4i)$$

3.2 Evaluation of Stability Derivatives by CFD Analyses

As noticeable in (4), within the framework of small perturbation theory, constructing dynamic model is reduced to the determination of the stability derivatives defined in the linearized equations of motion. Some stability derivatives in (4) are to be evaluated by using the techniques proposed in the flight dynamics or ship manoeuvrability (Etkin, 1982; Lewis et al., 1989). But since the configuration and layout of an AUV are generally quite different from those of aerial vehicle or surface ship, not all of stability derivatives appearing in (4) are to be determined by such techniques. Moreover, it is generally not easy to evaluate the stability derivatives deemed to dominate the calculated vehicle motion, for they are closely related to the damping and the energy transfer accompanied by the fluid flow (Lewis et al., 1989). The most commonly and widely employed approaches to evaluate the dominant stability derivatives are the wind tunnel test for aerial vehicles and the towing tank test for marine vehicles. Experimental approaches are however, implemented with huge experimental facility and many workforces, which require quite amount of expense even when the test is for a single model. In this article, we present a model-based approach for evaluating the dominant stability derivatives. In the approach, dominant stability derivatives are evaluated by means of the hydrodynamic loads, obtained as the results of CFD analyses. The basic idea of evaluating stability derivatives by the proposed approach is quite simple. When we are to evaluate the value of X_u defined at a reference speed of U_0 for example, we conduct CFD analyses repeatedly with the cruising speed of $U_0(1\pm\eta)$, where U_0 is the reference cruising speed and η is the perturbation ratio of U_0. By taking central difference approximation of X with respect to u by using the X values obtained at $U_0(1\pm\eta)$, we can derive X_u defined at U_0. However, while the majority of dominant stability derivatives are to be evaluated by this technique, there are other stability derivatives which are not. For such stability derivatives, estimation formulae proposed in the field of flight dynamics are modified and applied (McRuer et al., 1990; Etkin, 1982).

Figure 4 shows the grid system for evaluating the hydrodynamic loads by CFD analyses. In our CFD analyses, we used a solver called "Star-CD" (http://www.cdadapco.com/), developed by CD-adapco. The Star-CD is based on the finite difference numerical scheme and thus works with a structured grid system. In the aftbody of the R-One, geometric feature of the body surface is quite complicated due to the existence of tail fins. To generate a computationally robust structured grid system adapting to the geometric feature of the vehicle, we employed a grid generation technique called multi block method (Thomson, 1988). In the multi block method, entire grid system is subdivided into several local subgrid blocks, each of which shares the interfacing grids with the adjacent subgrid blocks.

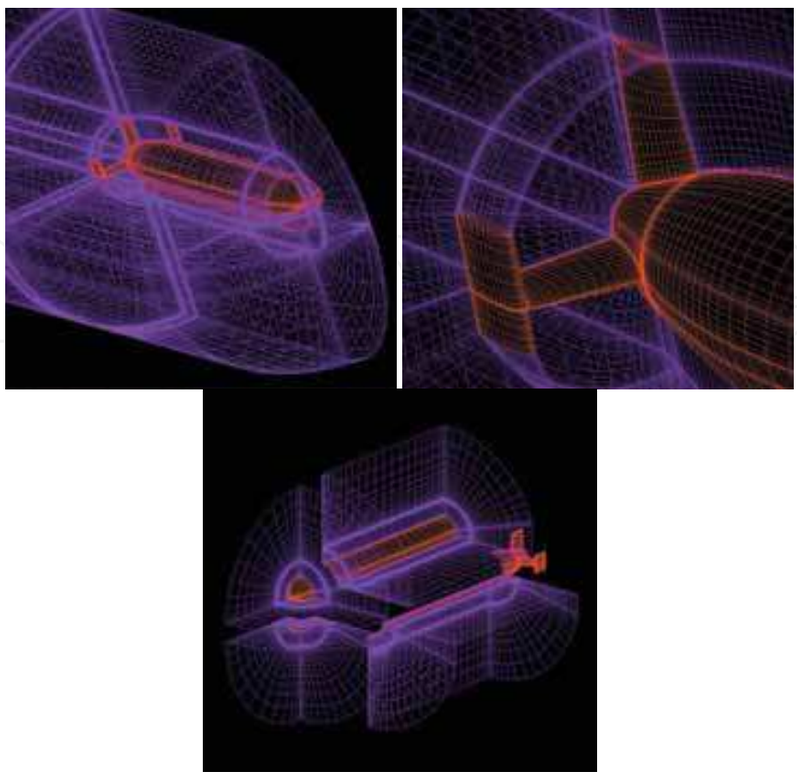

Fig. 4. Grid system for the CFD analyses of flow field around the body surface of the R-One. Due to the complicated surface geometry in the aftbody, entire grid system is completed by assembling individually generated subgrid blocks.

Figure 5 shows the pressure distribution with few selected streamlines along the body surface of R-One. By integrating the pressure over the entire body surface, hydrodynamic loads are obtained.

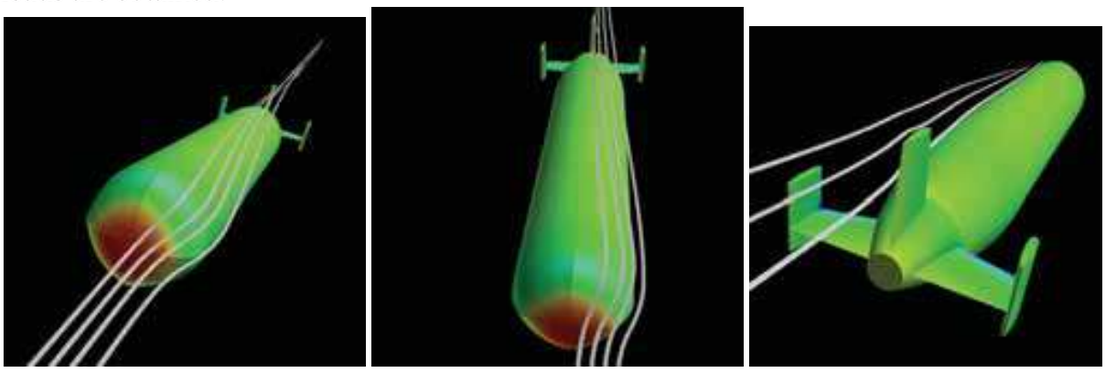

Fig. 5. Visualized results of a CFD analysis: Pressure distribution with few selected streamlines over the body surface of R-One.

By substituting all stability derivatives in (4) with their corresponding numerical values, dynamic model of R-One is completed. It is generally known and also noticeable from (4)

that according to the coupling relation, linearized equations of motion are to be split into two independent groups: the longitudinal equations including surge, heave, and pitch, and the lateral equations including sway, roll, and yaw (McRuer et al., 1990; Etkin, 1982). In Table 1, longitudinal and lateral stability derivatives appearing in (4) are summarized.

$X_{\dot{u}}$	(kg)	-237.65	Z_u	(kg/s)	-64.41
$Z_{\dot{w}}$	(kg)	-2819.64	Z_w	(kg/s)	-2819.64
$Z_{\dot{q}}$	(kg·m)	-25547.00	Z_q	(kg·m/s)	-11360.06
$M_{\dot{u}}$	(kg·m)	0.00	M_u	(kg·m/s)	0.00
$M_{\dot{w}}$	(kg·m)	-1928.80	M_w	(kg·m/s)	870.36
$M_{\dot{q}}$	(kg·m^2)	-153400.00	M_q	(kg·m^2/s)	-39351.25
X_u	(kg/s)	-728.73	Z_{δ_e}	(kg·m/s^2)	-3168.10
X_w	(kg/s)	33.36	M_{δ_e}	(kg·m^2/s^2)	-10974.31
X_q	(kg·m/s)	0.00			

Table 1a. Stability derivatives in the longitudinal equations for R-One.

$Y_{\dot{v}}$	(kg)	-237.65	Y_r	(kg·m/s)	3931.06
$Y_{\dot{r}}$	(kg)	-2819.64	L_v	(kg·m/s)	-515.99
$L_{\dot{v}}$	(kg·m)	-25547.00	L_p	(kg·m^2/s)	-1165.25
$L_{\dot{p}}$	(kg·m^2)	0.00	L_r	(kg·m^2/s)	1500.45
$L_{\dot{r}}$	(kg·m^2)	-1928.80	N_v	(kg·m/s)	-4054.37
$N_{\dot{v}}$	(kg·m)	-153400.00	N_p	(kg·m^2/s)	0.00
$N_{\dot{p}}$	(kg·m^2)	-728.73	N_r	(kg·m^2/s)	-13704.63
$N_{\dot{r}}$	(kg·m^2)	33.36	$Y_{\delta_{pr}}$	(kg·m/s^2)	-399.04
Y_v	(kg/s)	-1809.97	$L_{\delta_{pr}}$	(kg·m^2 /s^2)	0.00
Y_p	(kg·m/s)	0.00	$N_{\delta_{pr}}$	(kg·m^2 /s^2)	1677.38

Table 1b. Stability derivatives in the lateral equations for R-One.

3.3 Vehicle Motion Simulation

Equations (5a) and (5b) represent state-space forms of the longitudinal and the lateral equations of motion for R-One, completed by assigning the numerical values in Table 1 to corresponding stability derivatives in (4).

■ *Longitudinal Equations of Motion for R-One:*

$$\begin{bmatrix} \dot{u} \\ \dot{w} \\ \dot{q} \\ \dot{\theta} \end{bmatrix} = \begin{bmatrix} -0.1571 & 0.0072 & 0 & 0.0145 \\ -0.0103 & -0.4725 & 0.2456 & 0.0610 \\ 0.0001 & 0.0108 & -0.2420 & -0.0156 \\ 0 & 0 & 1 & 0 \end{bmatrix} \begin{bmatrix} u \\ w \\ q \\ \theta \end{bmatrix} + \begin{bmatrix} 0.0554 & 0 & 0 \\ 0 & 0.0027 & -0.2169 \\ 0 & -0.0001 & -0.0684 \\ 0 & 0 & 0 \end{bmatrix} \begin{bmatrix} n_m \\ n_v \\ \delta_e \end{bmatrix} \tag{5a}$$

■ *Lateral Equations of Motion for R-One:*

$$\begin{bmatrix} \dot{v} \\ \dot{p} \\ \dot{r} \\ \dot{\phi} \end{bmatrix} = \begin{bmatrix} -0.2097 & 0.0053 & -0.5388 & 0.0112 \\ -4.7444 & -11.2192 & 16.1215 & -23.6516 \\ -0.1185 & 0.0643 & -1.1931 & 0.1357 \\ 0 & 1 & 0 & 0 \end{bmatrix} \begin{bmatrix} v \\ p \\ r \\ \phi \end{bmatrix} + \begin{bmatrix} -0.0388 \\ -0.0948 \\ 0.0634 \\ 0 \end{bmatrix} \delta_{pr} \tag{5b}$$

By solving (5) in time domain with appropriate initial conditions and actuator inputs, motion responses of the R-One are computed. In the Inertial Navigation System (INS) installed in R-One, not only vehicle kinematics but also time sequences of the actuator inputs during an undersea mission are recorded. In Figs. 6 and 7, simulated vehicle trajectories are shown and compared with the actual vehicle trajectories which were recorded during the Teisi knoll survey mission (Ura et al., 2001). By applying the actual actuator inputs taken from the INS record to (5), simulated motion responses are computed producing the simulated vehicle trajectories. As noticeable from Figs. 6 and 7, the dynamic model of R-One implemented by our model-based approach provides the motion responses exhibiting sufficiently good similarity between the simulated and the actual vehicle trajectories.

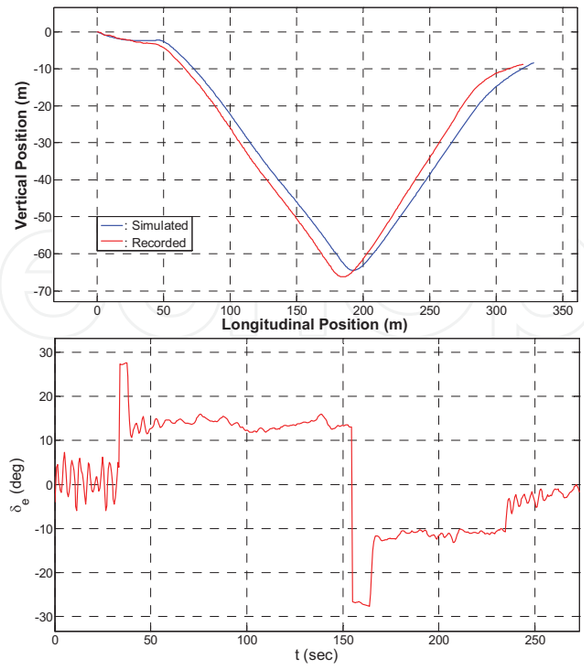

Fig. 6. Simulated and actual vehicle trajectories in vertical plane (top) generated from the corresponding actuator input (bottom).

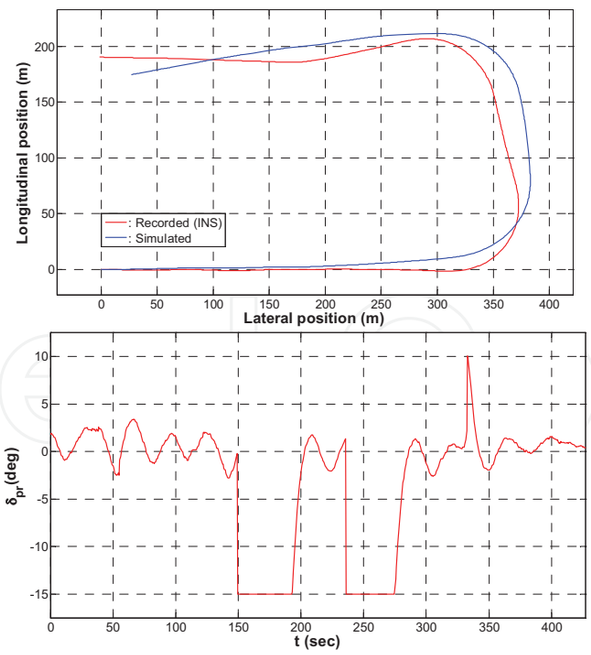

Fig. 7. Simulated and actual vehicle trajectories in horizontal plane (top) generated from the corresponding actuator input (bottom).

4. Tracking Control Design

The controller model selected to be implemented in the motion control system of R-One is based on the PID compensation. Needless to say, PID type controller is the most commonly and widely used controller for most artificial control systems. However in designing a PID controller, precise plant dynamics is an important prerequisite to ensure the acceptably good control performance. Deriving a precise plant dynamics is not easy in some cases. For this reason during the past two decades, a few significant attempts have been made to provide the controller models which do not require precise description of the plant model in its design. Neural network (NN) controllers based on the self-organizing map, or fuzzy logic controllers are the most famous ones in such attempts (Haykin, 1999). In order to derive a practically useful controller by NN or fuzzy however, we have to ensure huge diversity in training data. This is also a very difficult task in a real world problem, for in general we do not have any useful guideline to decide whether the prepared training data is biased or not. Moreover, since we have derived a fine dynamic model as shown in the previous section, we do not have any particular reason for choosing NN- or fuzzy-based controller model instead of the PID-based controller.

To change or keep the kinematic states of the vehicle, two independent low-level controls were implemented in the R-One: the depth (altitude) control for the longitudinal motion and the heading control for the lateral motion. Configurations of the depth and the heading controls are depicted in Fig. 8 and Fig. 9.

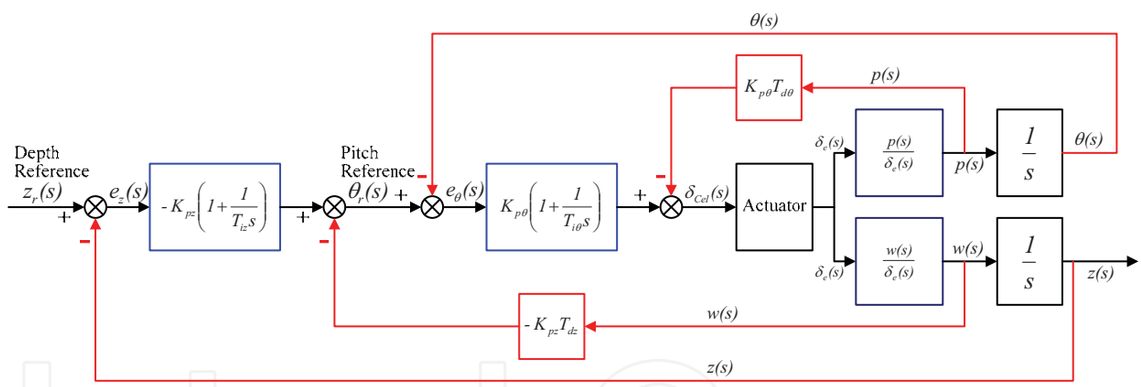

Fig. 8. Configuration of the depth (altitude) control system for R-One.

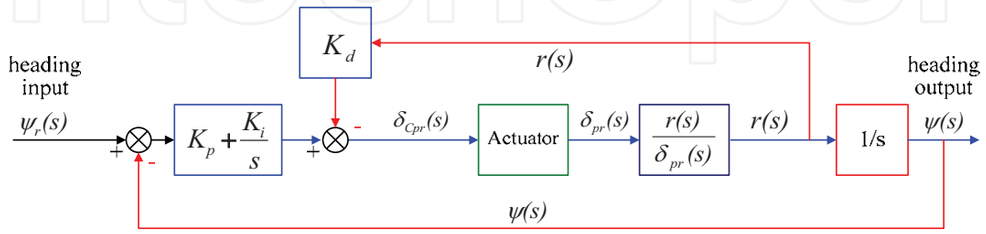

Fig. 9. Configuration of the heading control system for R-One.

In the model-based or computer-aided control system design, mathematical model describing the system behaviour should be prepared. To build up the mathematical models for the control systems shown in the Figs. 8 and 9, transfer functions of $p(s)/\delta_e(s)$, $w(s)/\delta_e(s)$, and $r(s)/\delta_{pr}(s)$ are extracted from (5). Then, the PID-tuning is carried out to determine the optimal values of controller gains from the standpoint of the system robustness and the swiftness in response. In determining the optimal gain values, we used the model-based control system design tool called "SISO Design Tool", offered by "Control System Toolbox" included in "Matlab" (The Mathworks Inc., 2001).

An example exhibiting the performance of the designed control systems is shown in Fig. 10. In the figure, it is clearly seen that the designed heading controller let the vehicle follow the heading reference with sufficient swiftness and small overshoot.

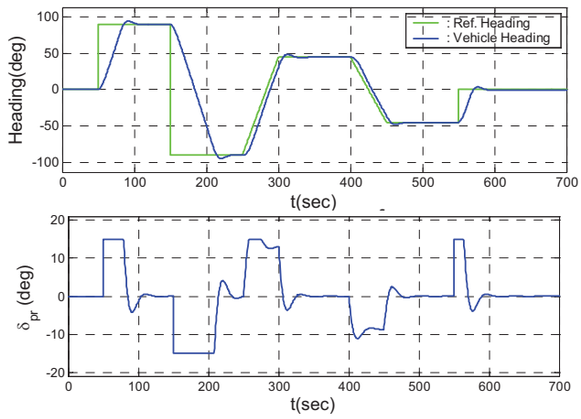

Fig. 10. Simulated heading tracking control (top) with corresponding actuator input (bottom).

5. Optimal Guidance of AUV

5.1 Background

The sea environment contains several disturbances such as surface wave, wind, and sea current. Among them, the sea current is known to be the most important disturbance for the dynamics of an underwater vehicle directly interacting with the vehicle motion (Lewis et al., 1989). Considering the guidance problem to make a vehicle transfer to a given destination in a region of sea current, it is quite natural that there happens navigation time difference according to the selection of an individual navigation trajectory. The problem of the minimum-time vessel guidance in a region of current flow interested people so long years ago as ancient Greece (Bryson & Ho, 1979). But since the problem requires minimization technique of the functionals, it hardly had been treated mathematically until the advent of the calculus of variations. On the basis of this mathematical tool, Bryson and Ho derived the minimum-time guidance law of a surface vessel in a region of a surface current flow. Though it is an optimal controller of explicit form described as an ordinary differential equation, to obtain its solution is not easy since it actually is so called a two point boundary value problem. As an ad hoc approach for the minimum-time navigation problem in a

linearly varying, shear flow like current distribution presented by Bryson and Ho, a graphical solution finding technique has been presented (Lewis & Syrmos, 1995). As is naturally expected however, such an approach is a problem specific one, lacking in universality in its applicability. Papadakis & Perakis (1990) treated the minimal time routing problem of a vessel moving in a region of wave environment. In their approach, by subdividing the navigation region into several subregions of different sea states, the path for the optimal routing is obtained by the dynamic programming approach. Aside from the difficulties in constructing a numerical solution procedure for their approach, it has a problem of significant solution dependency on the features of regional subdivision. As a completely discrete and nonlinear approach, the cell mapping technique was applied to derive the minimal time tracking trajectory to catch a moving target in a deterministic vortex field (Crespo & Sun, 2001). Though the cell mapping is quite suitable for the optimal control of strongly nonlinear systems, it also has the problem of significant solution dependency on the subdivision.

In this research, we propose a solution procedure to obtain the numerical solution of the optimal guidance law, achieving the minimum time navigation of an AUV in current fields. It is a simple but consistently applicable algorithm to the optimal navigation problem defined in any current filed, if only the distribution of which is deterministic. In applying the proposed procedure, a simulated navigation along any feasible trajectory terminated at the destination is required. We call this navigation the "reference navigation", because it is utilized as the reference in realizing the optimal navigation. As a fault-tolerable strategy in putting the proposed optimal navigation into practice, concept of the quasi-optimal navigation is introduced. The basic idea of the quasi-optimal navigation is quite simple, consisting of the on-site feedbacks of the optimal guidance revisions.

5.2 The Optimal Guidance Law

In this optimal guidance problem, we employed the guidance law presented by Bryson and Ho (1979), shown in (6).

$$\dot{\psi} = \sin^2\psi \frac{\partial v_c}{\partial x} + \frac{1}{2}\left(\frac{\partial u_c}{\partial x} - \frac{\partial v_c}{\partial y} \right) \sin 2\psi - \cos^2\psi \frac{\partial u_c}{\partial y} \tag{6}$$

In (6), ψ represents the vehicle heading, and u_c, v_c are x, y components of the sea current velocity. Though Bryson and Ho derived (6) on the assumption of the stationary flow condition, we have shown that it is also valid for time-varying currents, like tidal flows (Kim & Ura, 2009).

Equation (6) is a nonlinear ordinary differential equation of an unspecified vehicle heading $\psi(t)$. Though the solution of (6) seems to be readily obtainable by a suitable numerical scheme such as Runge-Kutta, there still remains a significant shortfall. While (6) defines an initial value problem, its solution cannot be obtained with an arbitrarily assigned initial heading. If we solve (6) with an arbitrary initial value of ψ, the vehicle following the solution of (6) as the heading reference does not arrive at the destination. It is because (6) is a two point boundary value problem in fact, correct initial value of which constitutes a part of the solution.

5.3 Numerical Solution Procedure

To obtain the solution of the two point boundary value problems, an iterative solution procedure is generally used such as "shooting" or "relaxation" (Press et al., 1992). Starting from an initial guess, solutions generated by these schemes are repeatedly adjusted to eliminate the discrepancies between the estimated and the desired boundary conditions at both endpoints. But these schemes strongly rely on the initial guess, inappropriate assignment of which may lead to a local solution or divergence. In this study, we present a numerical procedure to obtain the solution of (6), called "AREN", named as an acronym of Arbitrary REference Navigation". In applying the AREN, first we need to make a simulated navigation in which the vehicle travels following an arbitrary guidance law. In this navigation, traveling time for the vehicle to reach the destination should be recorded. This navigation we call the "reference navigation", and the corresponding traveling time the "reference navigation time", denoted by t_{f_ref}. The only requirement for the reference navigation is that the vehicle has arrived at the destination at the final state.

In AREN, to search for the correct initial heading numerically, the interval of $0 \sim 2\pi$ is divided by equally spaced N-1 subintervals as

$$\psi_0^{(i)} = i\Delta\psi \quad \text{for} \quad i=0,1,...N-1 \tag{7}$$

where $\Delta\psi = 2\pi/N$.

In (7), $\psi_0^{(i)}$ is (i)-th initial heading trial and $\Delta\psi$ is its increment, i.e. the interval of initial heading trials. Next, for an initial heading trial $\psi_0^{(i)}$, we solve (6) in time domain by a time marching scheme, which produces a simulated navigation starting from $\psi_0^{(i)}$. The navigation having produced here is called (i)-th "trial navigation" adjoining to $\psi_0^{(i)}$. Once the trajectory produced by a trial navigation passes through the destination, it is the optimal navigation since only if the optimal guidance law (6) with the correct initial heading let a vehicle reach the destination. Therefore, N trial navigations are possible candidates for the optimal navigation. In practice however, discretization error in initial heading trials causes the convergence error at the destination, so that the optimal navigation should be identified in an approximate manner.

For a navigation trajectory, we define the "minimum distance" which is the shortest distance between the destination and a trajectory. In Fig. 11, $l_{min}^{(k-1)}$, $l_{min}^{(k)}$, and $l_{min}^{(k+1)}$ represent the minimum distances between the destination and the trajectories generated by $(k-1)$-th, (k)-th, and $(k+1)$-th trial navigations, respectively.

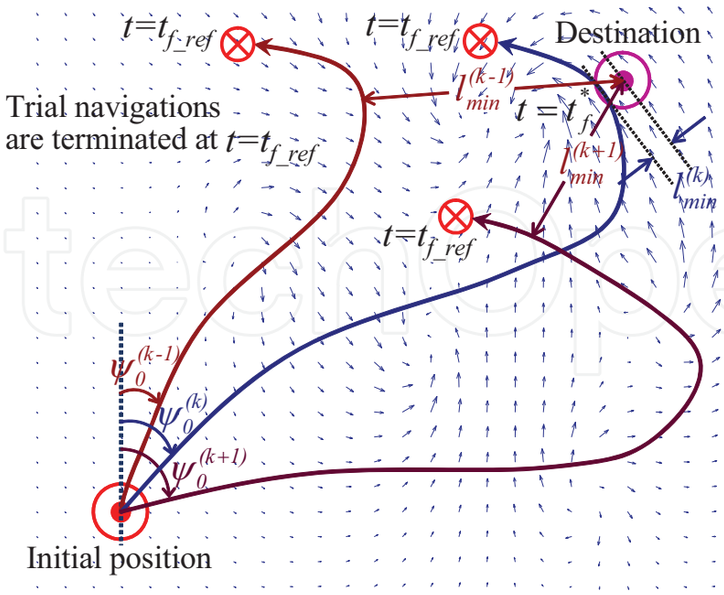

Fig. 11. Trial navigations starting from discrete initial headings. The approximate optimal navigation converging to destination is determined based on the minimum distances. Note that trial navigations are continued until $t = t_{f\_ref}$.

If the minimum distance of *(k)*-th trial navigation is smaller than any other minimum distance, and thus satisfies (8), we choose it as the optimal navigation because on its trajectory vehicle approaches the destination with the smaller deviation than any other trial navigation.

$$l_{min}^{(k)} \le l_{min}^{(i)} \quad \text{for } i=0,1,...N-1 \tag{8}$$

But in choosing the optimal navigation among the trials, there still remains a serious drawback. We have no idea how long we have to continue a trial navigation so as to determine its true minimum distance. Here comes the use of the reference navigation time prepared beforehand. It is apparent that the reference navigation is non-optimal, since it is the one following an arbitrary guidance law, only achieving the vehicle's arrival at the destination. Therefore, reference navigation time must be larger or equal to that of the optimal navigation as

$$0 < t_f^* \le t_{f\_ref} \tag{9}$$

where t_f^* represents navigation time by the optimal guidance. It should be noted here that by the minimum principle, once we have started a trial navigation with an initial heading close to optimal one, vehicle never fails to pass by the vicinity of the destination at the time smaller than t_{f_ref}. In other words, the reference navigation time qualifies to be the upper limits of the simulation times of the trial navigations in order to identify an optimal navigation among the trials, on the basis of the minimum distances. In Fig. 11, (*k*)-th trial navigation is picked up as the optimal navigation, since on its trajectory the vehicle marks the smallest minimum distance.

6. Optimal Navigation Examples

6.1 The Reference Navigation

As mentioned in the previous section, to implement the optimal guidance for vehicle navigation by AREN, it is necessary to make a reference navigation beforehand. The simplest guidance satisfying the vehicle's arrival at the destination may be the Proportional Navigation (PN). In PN, vehicle heading is continuously adjusted to let the line of sight direct toward the target. In our work, we employ PN as the reference navigation.

6.2 Optimal Navigation in a Shearing Flow

The first numerical example in this research is an optimal navigation in a current disturbance of the linear shear flow, taken from Bryson and Ho (1979). The current velocity in this problem is described by

$$u_c(x,y) = 0 \tag{10a}$$

$$v_c(x,y) = -U_c x/h \tag{10b}$$

where U_c and h are set to be 1.544 m/s and 100 m, respectively. Starting from the initial position at $(x_0, y_0) = (-186\ m, 366\ m)$, R-One is subjected to move the destination at the origin in this example. Due to its simplicity, the current distribution of (10) allows derivation of the analytic optimal guidance law expressed as

$$\frac{x}{h} = \csc\psi - \csc\psi_f \tag{11a}$$

$$\frac{y}{h} = \frac{1}{2}\left[\csc\psi_f(\cot\psi - \cot\psi_f) + \cot\psi(\csc\psi_f - \csc\psi) + \log\frac{\csc\psi_f - \cot\psi_f}{\csc\psi - \cot\psi}\right] \tag{11b}$$

where ψ_f is the vehicle heading at the final state.

Navigation trajectories are shown in Fig. 12. In the reference navigation by PN, significant adverse drift happens at initial stage, since within the region of $|x| > 100\ m$ current flow speed exceed the advance speed of the vehicle. Optimal guidance detours the vehicle across the upper half plane, taking advantage of the favorable current flow. Navigation times by PN and optimal guidance are 353.7 s and 739.2 s respectively, implying 52 % decrease in navigation time by the optimal guidance.

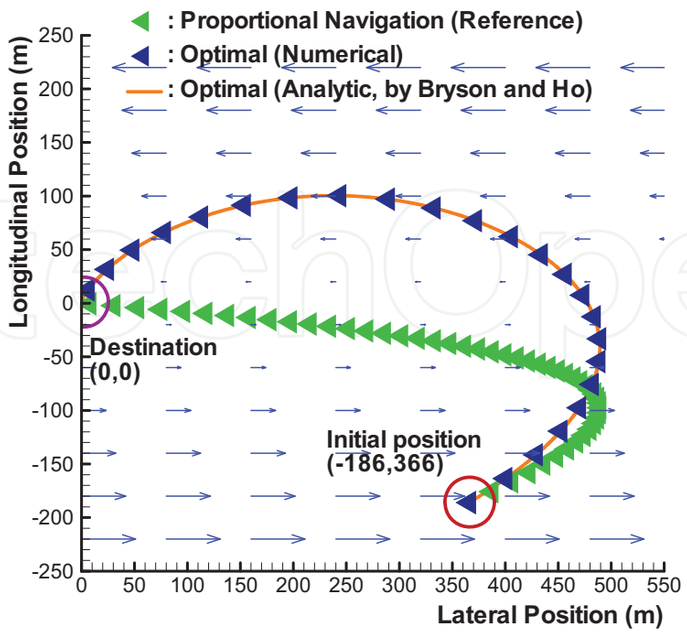

Fig. 12. Navigation trajectories in a linear shearing current flow.

6.3 Optimal Navigation in a Time-Varying Flow

The next numerical example is an optimal navigation in a time-varying current flow. In actual sea environments, for the most of currents the direction and the magnitude of their velocities change continuously like tidal flows. As mentioned previously, the optimal guidance law (6) is also valid for time-varying current flows as well as the stationary ones. Therefore, once the flow velocity distribution in a navigation region is described as a function of the position and time, our numerical scheme equally works and realizes the minimal time navigation.

Navigation trajectories of the R-One in an artificially made time-varying current are depicted in Fig. 13. As shown in the figure, near the middle of the navigation region, vehicle following the guidance of PN is temporarily failing to proceed toward the destination due to severe drift caused by local current flow of adverse direction. Occurrence of such a disadvantage is prevented from in the optimal navigation. By following the optimal guidance, the vehicle proceeds taking advantage of the favorable flows and avoids passing through the gradually changing region of strong adverse current flow. In Fig. 13, it should be noted that at 623.0 s, having released from the severe drift, R-One being controlled under the guidance of PN is about to restart toward the destination. At the same instant however, the optimal guidance has already made the vehicle arrive at the destination.

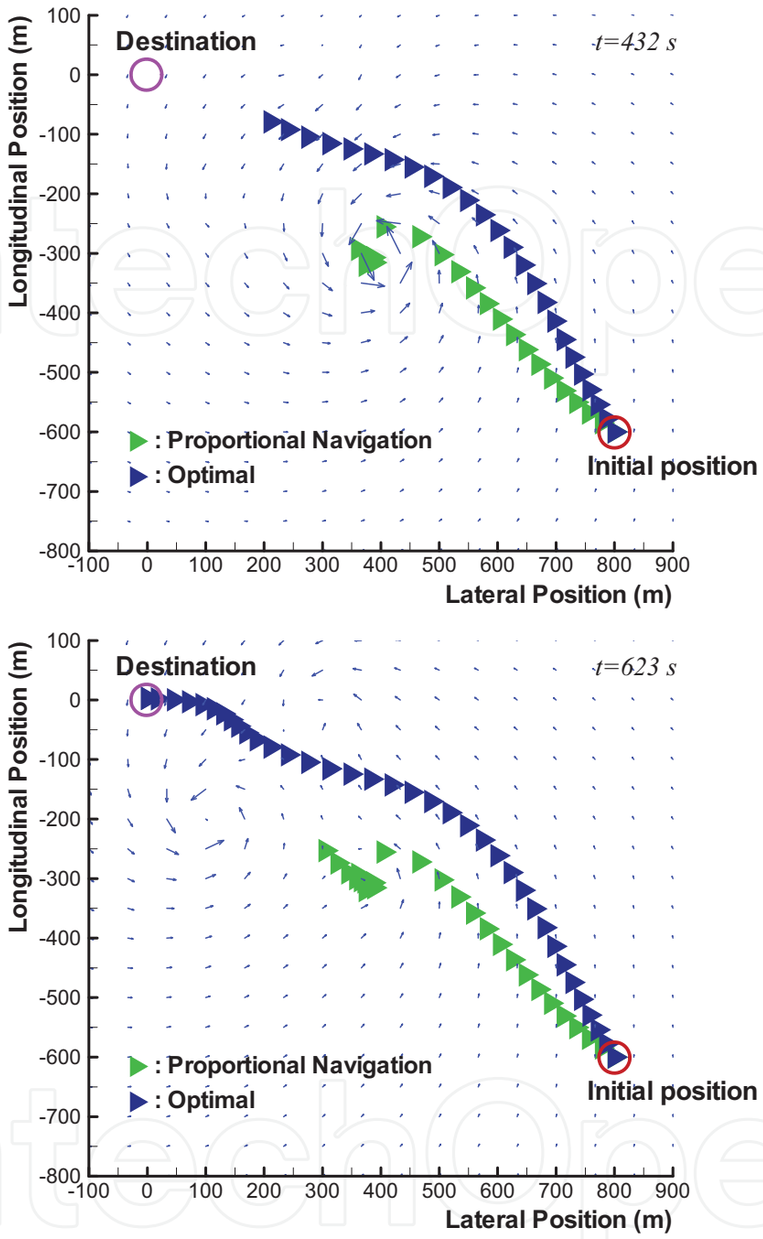

Fig. 13. Navigation trajectories in a time-varying current flow at t = 432 s (top), and t = 623 s (bottom).

6.4 Quasi-Optimal Navigation

The quasi-optimal navigation is a fail-safe strategy introduced to react to the failure in realizing the optimal navigation due to environmental uncertainties or temporal malfunctions in sensors and actuators. Suppose that a vehicle has failed in following the optimal trajectory due to one of the abovementioned problem. Not only has the navigation lost the optimality, but by following the current optimal guidance, vehicle is even unable to

arrive at the destination. According to the Bellman's principle of optimality (Lewis & Syrmos, 1995), once we have failed in tracking the optimal trajectory, the best policy we can take from then on is reconstructing and following the new optimal trajectory at the present state. The resulting trajectory is not optimal since it already has included the past non-optimal interval. But it is evidently the best trajectory we can take under present situation, so that we call the corresponding navigation the quasi-optimal navigation. In Fig. 14, optimal and quasi-optimal navigation trajectories in a time-varying current are shown.

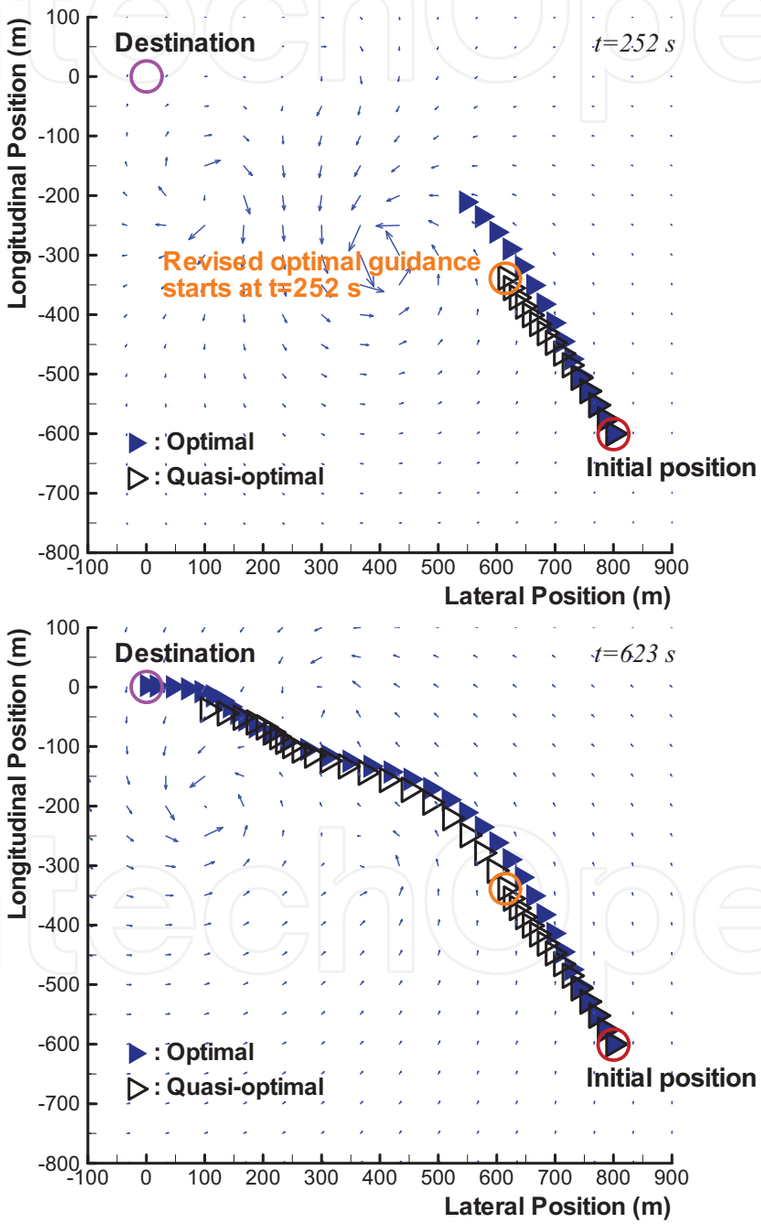

Fig. 14. Navigation trajectories in a time-varying current flow at t = 252 s (top), and t = 623 s (bottom).

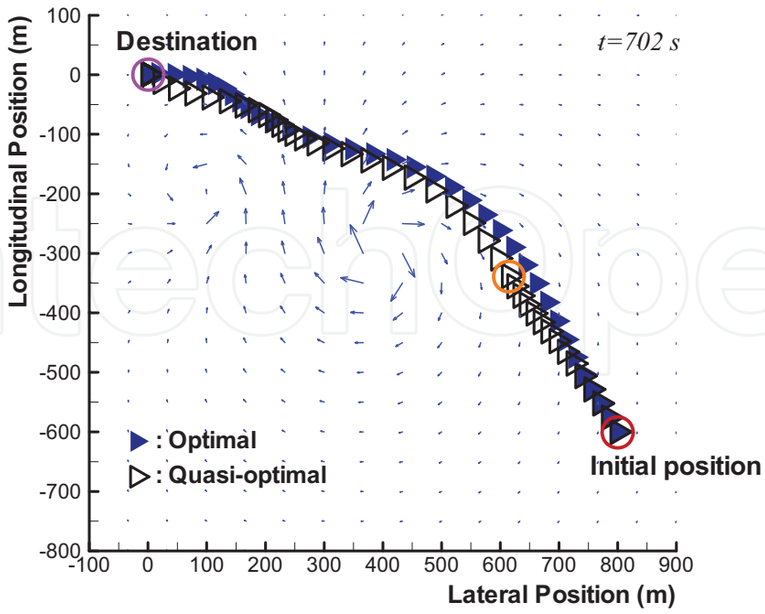

Fig. 14. Navigation trajectories in a time-varying current flow at t = 702 s (continued).

The current distribution in this example is the same one that we took in the previous one. In this example, while the optimal navigation is performed with the exact information on the current flow distribution, assuming a situation of incorrect localization due to sensor failure, mismatched current flow information is fed to the vehicle guidance controller in the quasi-optimal case. The time interval during which mismatched current flow information is taken in the quasi-optimal navigation is 0.0 s ~ 252.0 s. Starting at 252.0 s, revised optimal guidance on the basis of the correct current flow information achieves the quasi-optimal navigation. Fig. 15 shows the time sequence of the vehicle headings during the optimal and the quasi-optimal navigations.

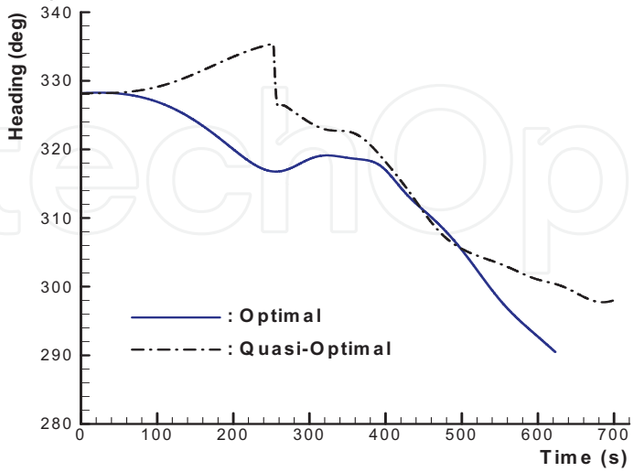

Fig. 15. Time sequence of vehicle headings.

As expected, the performance of the quasi-optimal navigation is not as high as that of the optimal one. While the optimal guidance completes the navigation at 623 s, the quasi-optimal one continues it until 702 s. Note that in Fig. 15, abrupt heading change occurs at 252.0 s during the quasi-optimal navigation.

7. Conclusions

In this article, a model-based synthetic approach to the following three main research fields in AUV design and development has been presented.

- Dynamic system modeling of AUV
- Motion control design and tracking control application
- Optimal guidance of AUV in sea currents

In the dynamic system modeling of the AUV R-One, we evaluated the hydrodynamic loads by using CFD analyses. Then by differentiating a hydrodynamic load with respect to a perturbed amount in vehicle kinematics, corresponding stability derivative were obtained. Using the stability derivatives evaluated, we built up the dynamic model of the R-One, which is characterized to be 6-D.O.F. (3 longitudinal (surge, heave, pitch) + 3 lateral (sway, roll, yaw)), linear, and Multiple-Input Multiple-Output (MIMO).
Depth and heading control systems are designed by employing controller models which are based on the PID compensations. In the PID-tuning, simulation models for the depth and the heading controls are exploited in determining the optimal gains.
Finally, concerning the guidance problem of AUVs moving in sea environmental disturbances, a procedure for obtaining the numerical solution of the optimal guidance law to achieve the minimum time navigation has been presented. The optimal heading is obtained as the solution of the optimal guidance law, which is fed to the heading control system as the heading reference. Reduced computational cost is one of the outstanding features of the proposed procedure. Numerical calculations of the optimal navigation examples presented in this article are completed within 10 minutes, on a single core 2.4 GHz windows XP platform. Moreover, unlike other path-finding algorithms such as dynamic programming or generic algorithm, our procedure does not require computation time increase for the time-varying problem.
As a fail-safe strategy in realizing the optimal navigation, the concept of the quasi-optimal guidance has been proposed. The fact that there actually are several possible actions lessening the chance of achieving optimality emphasizes the practical importance of the quasi-optimal navigation strategy.
We have not considered the problem of unknown or nondeterministic currents. Our approach cannot be applied to an entirely unknown environment. For a sea region including partially or coarsely defined current however, an estimated distribution can be built via interpolation and extrapolation. The estimation possibly contains more or less uncertainty. Notably it is the quasi-optimal strategy that can cope with the environmental uncertainty. When the uncertainty in the estimation is considerably significant, convergence may not be guaranteed, however.

8. References

Etkin, B. (1982). *Dynamics of Flight - Stability and Control*, John Wiley & Sons, ISBN 0-471-08936-2, New York

McRuer, D.; Ashkenas, I. & Graham, D. (1990). *Aircraft Dynamics and Automatic Control*, Princeton University Press, ISBN 978-0691024400, New Jersey

Lewis, E. V. (Ed., 1989). *Principles of Naval Architecture Vol III, Motions in Waves and Controllability*, The Society of Naval Architects and Marine Engineers, ISBN 0-939773-02-03, New Jersey.

Haykin, S. (1999). *Neural Networks*, Prentice Hall, ISBN 0-13-908385-5, New Jersey

The Mathworks Inc. (2001). *Control System Toolbox User's Guide*, The Mathworks Inc., Natick

Bryson, A. E. & Ho, Y. C. (1975). *Applied Optimal Control*, Taylor & Francis, ISBN 0-89116-228-3, Levittown

Lewis, F. L. & Syrmos, V. L. (1995). *Optimal Control*, John Wiley & Sons, ISBN 0-471-03378-2, New York

Press, W. H.; Teukolsky, S. A.; Vetterling, W. T. & Flannery, B. P. (1992). *Numerical Recipes in Fortran*, Cambridge University Press, ISBN 0-521-43064-X, Cambridge

Kim, K. & Ura, T. (2008). Optimal and Quasi-Optimal Navigations of an AUV in Current Disturbances, *Proceedings of IEEE/RSJ 2008 International Conference on Intelligent Robots and Systems (IROS2008)*, pp. 3661-3667, Nice, September 2008

Ura, T. ; Obara, T. ; Takagawa, S. & Gamo, T. (2001). Exploration of Teisi knoll by Autonomous Underwater Vehicle R-One Robot, *Proceedings of MTS/IEEE OCEANS2001*, pp. 456-461, Honolulu, November 2001

Alvarez, A.; Caiti, A. & Onken, R. (2004). Evolutionary Path Planning for Autonomous Underwater Vehicles in a Variable Ocean. *IEEE Journal of Oceanic Engineering*, Vol. 29, No. 2, (April 2004) 418-429

Thomson, J. F. (1988). A composite grid generation code for general 3D regions – the Eagle code. *AIAA Journal*, Vol. 26, No. 3, (March 1988) 1-10

Papadakis, N. A. & Perakis, A. N. (1990). Deterministic Minimal Time Vessel Routing. *Operations Research*, Vol. 38, No. 3, (May 1990) 426-438

Crespo, L. G. & Sun, J. Q. (2001). Optimal Control of Target Tracking with State Constraints via Cell Mapping. *Journal of Guidance, Control, and Dynamics*, Vol. 24, No. 5, (September 2001) 1029–1031

Kim, K. & Ura, T. (2009). Optimal Guidance for Autonomous Underwater Vehicle Navigation within Undersea Areas of Current Disturbances. *Advanced Robotics*, Vol. 23, No. 5, (April 2009) 601–628

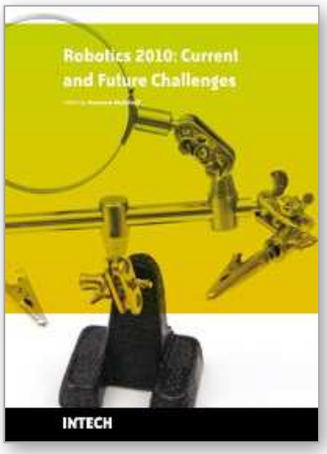

Robotics 2010 Current and Future Challenges

Edited by Houssem Abdellatif

ISBN 978-953-7619-78-7
Hard cover, 494 pages
Publisher InTech
Published online 01, February, 2010
Published in print edition February, 2010

Without a doubt, robotics has made an incredible progress over the last decades. The vision of developing, designing and creating technical systems that help humans to achieve hard and complex tasks, has intelligently led to an incredible variety of solutions. There are barely technical fields that could exhibit more interdisciplinary interconnections like robotics. This fact is generated by highly complex challenges imposed by robotic systems, especially the requirement on intelligent and autonomous operation. This book tries to give an insight into the evolutionary process that takes place in robotics. It provides articles covering a wide range of this exciting area. The progress of technical challenges and concepts may illuminate the relationship between developments that seem to be completely different at first sight. The robotics remains an exciting scientific and engineering field. The community looks optimistically ahead and also looks forward for the future challenges and new development.

How to reference

In order to correctly reference this scholarly work, feel free to copy and paste the following:

Kangsoo Kim and Tamaki Ura (2010). A Model-Based Synthetic Approach to the Dynamics, Guidance, and Control of AUVs, Robotics 2010 Current and Future Challenges, Houssem Abdellatif (Ed.), ISBN: 978-953-7619-78-7, InTech, Available from: http://www.intechopen.com/books/robotics-2010-current-and-future-challenges/a-model-based-synthetic-approach-to-the-dynamics-guidance-and-control-of-auvs

INTECH
open science | open minds

InTech Europe
University Campus STeP Ri
Slavka Krautzeka 83/A
51000 Rijeka, Croatia
Phone: +385 (51) 770 447
Fax: +385 (51) 686 166
www.intechopen.com

InTech China
Unit 405, Office Block, Hotel Equatorial Shanghai
No.65, Yan An Road (West), Shanghai, 200040, China
中国上海市延安西路65号上海国际贵都大饭店办公楼405单元
Phone: +86-21-62489820
Fax: +86-21-62489821

IntechOpen